

Chimeric green fluorescent protein-aequorin as bioluminescent Ca^{2+} reporters at the single-cell level

Valérie Baubet*, Hervé Le Mouellic*, Anthony K. Campbell†, Estelle Lucas-Meunier‡, Philippe Fossier‡, and Philippe Brûlet*[§]

*Unité d'Embryologie Moléculaire, Unité de Recherche Associée 1947, Centre National de la Recherche Scientifique, Institut Pasteur, 25 rue du docteur Roux, 75724 Paris Cedex 15, France; †Department of Medical Biochemistry, University of Wales College of Medicine, Heath Park, Cardiff CF4 4XN, United Kingdom; and ‡Laboratoire de Neurobiologie Cellulaire et Moléculaire, UPR 9040 Centre National de la Recherche Scientifique, avenue de la Terrasse, 91198 Gif-sur-Yvette Cedex, France

Communicated by François Jacob, Institut Pasteur, Paris, France, April 14, 2000 (received for review February 1, 2000)

Monitoring calcium fluxes in real time could help to understand the development, the plasticity, and the functioning of the central nervous system. In jellyfish, the chemiluminescent calcium binding aequorin protein is associated with the green fluorescent protein and a green bioluminescent signal is emitted upon Ca^{2+} stimulation. We decided to use this chemiluminescence resonance energy transfer between the two molecules. Calcium-sensitive bioluminescent reporter genes have been constructed by fusing green fluorescent protein and aequorin, resulting in much more light being emitted. Chemiluminescent and fluorescent activities of these fusion proteins have been assessed in mammalian cells. Cytosolic Ca^{2+} increases were imaged at the single-cell level with a cooled intensified charge-coupled device camera. This bifunctional reporter gene should allow the investigation of calcium activities in neuronal networks and in specific subcellular compartments in transgenic animals.

Calcium is implicated in the regulation of a great variety of intracellular processes (1). Several techniques are most commonly used for intracellular Ca^{2+} monitoring. Patch-clamp and Ca^{2+} selective microelectrodes give cumulative measurements of Ca^{2+} fluxes in a restricted number of cells. On the other hand, intracellular Ca^{2+} concentration dynamics in large populations of cells can be visualized with fluorescent probes (2). Genetic tools could provide new methods for Ca^{2+} monitoring. Two groups of genetic Ca^{2+} probes are presently available. The first category uses the principle of fluorescence resonance energy transfer (FRET) between two variants of the green fluorescent protein (GFP). The two GFPs are covalently linked by a calmodulin binding sequence alone or in combination with calmodulin so that intramolecular FRET does (3) or does not (4) occur in response to Ca^{2+} influx. The second category is composed of bioluminescent proteins such as aequorin (5, 6). The active protein is formed in the presence of molecular oxygen from apoaequorin (189 aa) and its luciferin, coelenterazine (M_r 423) (7). The binding of Ca^{2+} to aequorin, which has three EF-hand structures characteristic of Ca^{2+} binding sites, induces a conformational change resulting in the oxidation of coelenterazine via an intramolecular reaction. Moreover, the coelenteramide so produced is in an excited state and blue light (λ_{max} , 470 nm) is emitted when it returns to its ground state (8). Such a bioluminescent genetic marker presents the advantage over Ca^{2+} -sensitive fluorescent dyes of being easily targeted to specific cells and in subcellular compartments with appropriate regulatory elements and peptide signals (9). The bioluminescent process does not require light excitation like fluorescent probes or proteins and thus does not induce autofluorescence, photobleaching, and biological degradation problems. Furthermore, aequorin is not toxic, does not bind other divalent cations, and does not interfere with the intracellular Ca^{2+} concentration buffer system even when microinjected at high concentrations.

Its low affinity for Ca^{2+} ($K_d = 10 \mu\text{M}$) is probably responsible for this and makes aequorin a good sensor in the range of biological Ca^{2+} concentration variations. Although providing a good ratio of signal over background, aequorin signals are very difficult to detect because of aequorin's low light quantum yield, that is the number of emitted photons per protein that bind Ca^{2+} . In the jellyfish *Aequorea victoria* from which aequorin has been isolated (10), the protein is associated with the GFP (11). After Ca^{2+} binding, the energy acquired by aequorin is transferred from the activated oxyluciferin to GFP without emission of blue light. The GFP acceptor fluorophore is excited by the oxycelenterazine through a radiationless energy transfer. Then, a green light (λ_{max} , 509 nm) is emitted when the excited GFP returns to its ground state (12).

Such intermolecular radiationless energy transfer is not unusual in bioluminescence and already has been shown to increase the quantum yield of the bioluminescent process in *Renilla*, another coelenterate (13). The gain measured *in vitro* ranges from 3- to 5-fold (14). It is possible to reconstitute *in vitro* the *Renilla* system and obtain the spectral shift with low equimolar concentrations of its components because the luciferase and the GFP bind together (14). In the *Aequorea* system, binding between purified photoprotein and GFP does not occur in solution, even when present at high concentrations (15). *In vivo*, energy transfer occurs because of the high concentration of GFP. It can be obtained *in vitro* through the coadsorption of aequorin and GFP on DEAE cellulose membranes (15). The Förster equation shows that the efficiency of this process depends on several conditions described in the case of fluorescence resonance energy transfer. The emission spectrum of the donor must have the greatest overlap with the excitation spectrum of the acceptor. The energy transferred also strongly depends on the geometry, in particular the relative orientation and distance of the two dipoles and modulated by their respective motion (16).

The aim of our study is to develop a dual reporter gene combining properties of Ca^{2+} sensitivity and fluorescence of aequorin and GFP, respectively. The fusion protein, which can be detected with classical epifluorescence, could be used to monitor calcium activities. The configuration of our molecules increases their overall turnover and allows an efficient intramolecular chemiluminescence resonance energy transfer (CRET). As a result, the quantum yield of aequorin appears to be higher. In this paper, we show that physiological calcium

Abbreviations: GFP, green fluorescent protein; EGFP, enhanced GFP; CRET, chemiluminescence resonance energy transfer; CCD, charge-coupled device; RLU, relative light unit.

[§]To whom reprint requests should be addressed. E-mail: pbrulet@pasteur.fr.

The publication costs of this article were defrayed in part by page charge payment. This article must therefore be hereby marked "advertisement" in accordance with 18 U.S.C. §1734 solely to indicate this fact.

signals can be visualized in single neuroblastoma cells with an intensified charge-coupled device (CCD) camera. Other constructs described here target the fusion protein to the neurite membrane.

Materials and Methods

Construction of GFP-Aequorin Fusion Proteins. All of the constructs were made in the pEGFP-C1 vector (CLONTECH). The enhanced GFP (EGFP) gene is codon-optimized for maximal expression in mammalian cells. It also contains two mutations in the chromophore, F64L and S65T, which modify the excitation spectra and enhance fluorescence intensity (17). We further substituted valine 163 of the EGFP by alanine, by using single-strand mutagenesis, to improve the proper folding of the protein and increase the fluorescence at 37°C (18, 19). The aequorin coding sequence, a generous gift by M.-T. Nicolas (Institut National de la Santé et de la Recherche Médicale, France), has been fused in-frame at the 3' end of the EGFP gene in the *Bgl*III/*Sal*I sites of pEGFP-C1. Seven codons were modified for a better expression in mammalian cells by means of site-directed mutagenesis using PCR with overlap extension. Then, complementary oligonucleotides, 5'-CCGGCGGGAGCGGATCCG-GCGGCCAGT-3' and 5'-CCGGACTGGCCGCGGATC-CGCTCCCG-3' were inserted at the *Bsp*EI site in the 15-bp sequence between GFP and aequorin. Conservation of the *Bsp*EI site at only one end allowed sequential addition of 1–5 linker sequences (pG1A–pG5A).

Two additional fusion constructs were made in pG5A with a synaptic protein, synaptotagmin I of which the cDNA plasmid was a generous gift of M. Fukuda, Molecular Neurobiology Laboratory, Tsukuba Life Science Center (RIKEN), Japan. Sequences encoding for either the entire ORF or the first 134 N-terminal aa, comprising the transmembrane domain of the protein, were fused in-frame at the 5' end of the GFP-aequorin gene.

Cell Culture and Transfection. Neuroblastoma cells (Neuro2A, mouse) were grown in DMEM (Life Technologies, Paisley, U.K.; GIBCO) supplemented with 10% (vol/vol) heat-treated FCS, 2 mM glutamine (Life Technologies; GIBCO), and 100 units of streptomycin-penicillin (Life Technologies; GIBCO). The culture was incubated at 37°C in a humidified atmosphere containing 8% CO₂ and transiently transfected by using either the calcium phosphate technique or the FuGENE 6 transfection reagent (Roche, Diagnostics).

In Vitro Ca²⁺-Sensitive Chemiluminescence and CRET Activities. Cells were harvested 48 h after transfection in 250 μl of 10 mM β-mercaptoethanol, 4 mM EDTA, 5 μM coelenterazine in PBS at 4°C over 2–4 h. Cells were rinsed in 1 mM EDTA in PBS and harvested in 400 μl of hypoosmotic buffer (20 mM Tris·HCl, pH 7.5/5 mM EDTA/5 mM β-mercaptoethanol with a protease inhibitor mixture according to the manufacturer, complete, mini EDTA-free; Roche Diagnostics), for 30 min to 1 h at 4°C. The cell membrane was broken by passing through a 30-gauge needle, and the cellular extract was obtained after microcentrifugation at 13,000 rpm for 1 h at 4°C. The supernatant was harvested for all constructions but SG5A for which the membrane pellet was further resuspended. Calcium sensitivity chemiluminescent activity was measured in a luminometer (Lumat LB95501 E&EG Berthold, Wildbad, Germany). Aliquots (10 μl) were placed in a sample tube (with 90 μl of 10 mM Tris·HCl, pH 7.5) in the luminometer, and the light intensity expressed in relative light units (RLUs) was measured after the injection of 100 μl of 50 mM CaCl₂/10 mM Tris·HCl, pH 7.5 solution.

For CRET measurements, aliquots of extracts from transfected cells were placed in a reservoir chamber and brought into contact with an optic fiber bundle attached to a photon counting

camera (Photek three-microchannel plate intensified CCD camera: Photek 216, East Sussex, U.K.). Before capture of signals, light passes through a monochromator, allowing the spectral analysis of emitted photons. The acquisition begins 20 sec before injection of CaCl₂ and carries on 40 sec after injection of the CaCl₂ solution (50 mM). For green/blue photon ratio determinations, the same procedure was followed but in that case the system measured the light emitted through blue (450 nm) and green (500 nm) filters after a beam-splitter.

GFP Fluorescence and Immunolocalization. Neuro2A cells were fixed 48 h after transfection in 4% paraformaldehyde in PBS, pH 7.4, rinsed in PBS, and mounted. GFP fluorescence was visualized under a confocal laser scanning microscope (Zeiss), which uses an argon-krypton laser operating in multiline mode or an Axiophot microscope with an epiluminescent system (Zeiss). For immunolocalization of the targeted GFP-aequorin, fixed cells were pretreated with 50 mM NH₄Cl in PBS, pH 7.4, for 5 min at room temperature and permeabilized in 2% BSA/0.02% Triton/goat serum solution in PBS for 1 h. Antibody against synaptotagmin (StressGen Biotechnologies, Victoria, Canada, SYA-130) then was applied over 2–4 h. Cells then were rinsed in PBS and incubated in 2% BSA/0.02% Triton in PBS with secondary antibody diluted at 1/100 (tetramethylrhodamine B isothiocyanate-conjugated antibody). Cells then were washed in PBS and mounted.

Single Cells' Bioluminescence Detection. Forty-eight hours after transfection, cells were rinsed in 124 mM NaCl/5 mM KCl/15 mM Hepes, pH 7.4/5 mM NaHCO₃/1 mM NaH₂PO₄/0.5 mM MgSO₄/1.5 mM CaCl₂/5.5 mM glucose and later incubated in the same buffer without CaCl₂ with 5 μM coelenterazine to reconstituted aequorin, for 2–4 h at 37°C and then rinsed. Calcium signals were visualized with a modified Olympus upright microscope fitted with a BH2-RFCA epifluorescence unit recorded through a plan ×40 Olympus long working distance water-immersion lens (numerical aperture 0.7). GFP fluorescence allowed us to choose the recording area on transfected cells. The excitation lamp was shut off and the gain of the camera was increased. Images were integrated every sec with a cooled Photonic Science (Robertsbridge, U.K.) extended ISIS video camera. Each profile in Fig. 4 represents the amount of light emitted over the area that we defined around the soma of individual cells with Axon Imaging Workbench 2214 software. Intensities of fluorescence and CRET activity were translated in scaled pseudocolors. Controls were made with Fluo-3 AM on mock-transfected Neuro2A cells to check the experimental conditions.

Results and Discussion

GFP-Aequorin Fusion Proteins as Ca²⁺-Activated Reporter Genes. We have chosen to construct a fusion protein with aequorin and GFP to increase the quantum yield of Ca²⁺-induced bioluminescence. This activity cannot be increased simply by coexpressing GFP with aequorin (data not shown). A thermoresistant GFP (Gm) was fused in-frame with the NH₂-terminal region of apoaequorin (Fig. 1), because the C-terminal proline residue has been shown to be implicated in the Ca²⁺-activated bioluminescent process (20). We have made different constructs with increasing size of linker between GFP and apoaequorin. The shortest spacer was formed by 5 aa and the longest by 50 aa (Fig. 1). All of the fusion proteins showed a better Ca²⁺-triggered bioluminescent activity than aequorin alone. The increases of light-emitting activity ranged from 19 to 65 times (Table 1) possibly because of greater protein stability. Recombinant apoaequorin is unstable within the cytosol, with a half-life of approximately 20 min (21). In contrast, GFP is a very stable protein and probably stabilizes apoaequorin in the chimeric proteins. The turnover times of the different cytosolic proteins were estimated on transient expres-

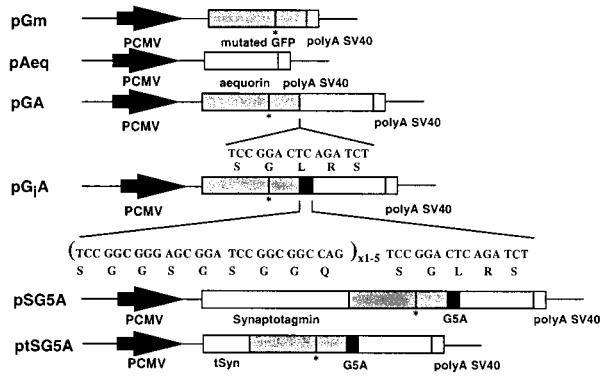


Fig. 1. Schematic map of the different constructions. All of the constructs were under the control of the human cytomegalovirus promoter (PCMV). * indicates the position of the Val-163-Ala mutation. In pGA, the coding sequences of GFP and aequorin are separated by five codons. One to five linkers (in brackets) have been added in pGiA where i is the number of linker. Linkers were oriented so as to encode a 9-aa repeat. Complete synaptotagmin I or its transmembrane part (tSyn) were fused in-frame with the G5A. SV40, simian virus 40.

sion in COS7 cells by treatment with puromycin (50 $\mu\text{g/ml}$) for 6 h. Over this period, most fusion proteins presented a 30% decrease of activity compared with the 80% loss of apoaequorin when alone (data not shown). We also noticed that, *in vitro*, the hybrid proteins were more sensitive than aequorin alone. G5A gives a significant signal over background with Ca^{2+} concentration as low as 38 nM whereas aequorin needs 28 times more calcium ($\approx 1 \mu\text{M}$) to yield a comparable signal (data not shown). Energy transfer also may improve the quantum yield of GFP-aequorin, allowing a more efficient calcium ion detection. To discriminate among the factors contributing to the higher light emission, it will be necessary to study the relaxation mechanisms of the GFP fluorescent excited state on purified hybrid proteins.

Optimization of the Energy Transfer by Inserting a Spacer Between GFP and Apoaequorin. A nonradiative energy transfer between the excited oxyluciferin and the GFP chromophore will strongly depend on their overall geometry and their respective motions. We therefore have designed a linker principally composed of serine and glycine residues to intercalate a flexible element of variable length. The ratio of green and blue photons emitted upon Ca^{2+} triggering has been measured on cellular extracts prepared 48 h after transient transfection of Neuro2A cells. The photons emitted through a beam-splitter were counted after passing appropriate filters. Covalent linking of GFP to aequorin (GA) significantly modified the wavelength of maximum light emission (Fig. 2), thereby demonstrating intramolecular energy transfer. The ratio of green over blue light (500/450 nm) was

Table 1. Ca^{2+} -induced chemiluminescence activities

Name	Mean \pm SEM, RLU $\times 10^6/10$ units β -gal
pA	0.15 (0.10; 0.21)
pGA	10.01 \pm 4.4
pG1A	2.96 (3.39; 2.53)
pG2A	8.39 (9.54; 7.23)
pG4A	7.78 (12.02; 3.53)
pG5A	8.15 \pm 1.72
ptSG5A	3.89 (2.80; 4.97)

SEM is indicated when more than two measurements were made. Otherwise the two measurements are given. β -gal, β -galactosidase.

further raised from 3 to around 7 by adding 1–5 linkers (Fig. 2, CRET). Preliminary measurement indicates that this ratio can reach almost 11 with SG5A probably because of the accumulation of the fusion protein anchored to the membranes (see *Materials and Methods*). Spectral emissions of the different constructs also were analyzed by using a monochromator. Aequorin showed a broad spectrum with maximum wavelength at 474 ± 6.9 nm and a bandwidth, corresponding to the distance between low and high wavelengths at 50% values of the maximum emission, at 108.3 ± 20.1 nm (Fig. 2). There was a clear shift toward the green in the peak emission of the GFP-aequorin constructions ranging from 506.7 ± 1.2 nm to 514.1 ± 3.4 nm. Increasing the length of the linker further affected the sharpness of the spectrum, as indicated by the narrower bandwidths, 88.4 ± 9.4 nm and 56.0 ± 3.3 nm, for pGA and pG5A, respectively. There was no evidence of a bimodal spectrum with any of the pG1A–pG5A constructs, indicating an optimal transfer that could be incomplete in the case of pGA. When the spacer between GFP and aequorin is longer than 14 aa, the donor and the acceptor dipoles probably have more freedom to be in a configuration favorable for optimum intramolecular energy transfer. Our system yields an efficiency comparable to the intermolecular CRET measured *in vivo* (22, 23) and provides a convenient model for the biophysical studies of radiationless energy transfer mechanisms.

Cellular Localization and Targeting of GFP-Apoaequorin. We have checked the cellular localization of the GFP-apoaequorin constructs. Fig. 3 illustrates GFP activity 48 h after transient transfection in Neuro2A cells. Expression of the mutant GFP alone (Gm) showed homogenous fluorescence in the cytosol as well as in the nucleus as expected because GFP is a small protein that can diffuse into the nucleus. Mutation V163A remarkably improves the fluorescence signal and reduces photobleaching when compared with the original EGFP (data not shown), probably owing to a higher concentration of properly folded protein. An even distribution also is observed for all of the GFP-apoaequorin constructions in Neuro2A cells (Fig. 3A–D) as well as in COS-7 cells. Bright spots often appeared in the cytosol with fusion proteins having the shortest linkers: GA, G1A, and G2A. These spots were less frequent with G4A and never observed with Gm and G5A. High concentrations of proteins expressed during transient transfections could induce the aggregation of GFP (24), which also is going to be influenced by the presence of the aequorin protein and the distance separating them.

The GFP-apoaequorin also has been targeted to the neurotransmitter vesicles with a complete or a partial synaptotagmin I molecule. Synaptotagmin I is a transmembrane protein of synaptic vesicles and is implicated in neurotransmitter exocytosis (25). For imaging calcium microdomains in presynaptic compartments, the signal should be more accurate than if evenly distributed in the cytoplasm of neurons. In a three-part fusion protein, SG5A (Fig. 1), the complete coding sequence of synaptotagmin I has been put in-frame upstream of G5A. In this case, GFP fluorescence is superimposable with synaptotagmin immunostaining but is also visible at the cellular surface (Fig. 3E). In neurons (26) and Neuro2A cells, synaptotagmin I is localized in neuronal processes but is undetectable in plasma membranes probably because the dynamic mechanisms of exocytosis are followed by rapid endocytosis. When GFP-apoaequorin is fused with only the N-terminal part of synaptotagmin including the transmembrane domain but lacking the cytoplasmic domain (tSG5A, Fig. 1) a strong fluorescence is restricted to the cytosol (Fig. 3F). The punctate labeling suggests that this protein is locked into the trans-Golgi system. The correct targeting of our three-part fusion molecule does not occur with tSG5A and appears to be slowed down in the case of SG5A. When fused to the complete synaptotagmin protein, the

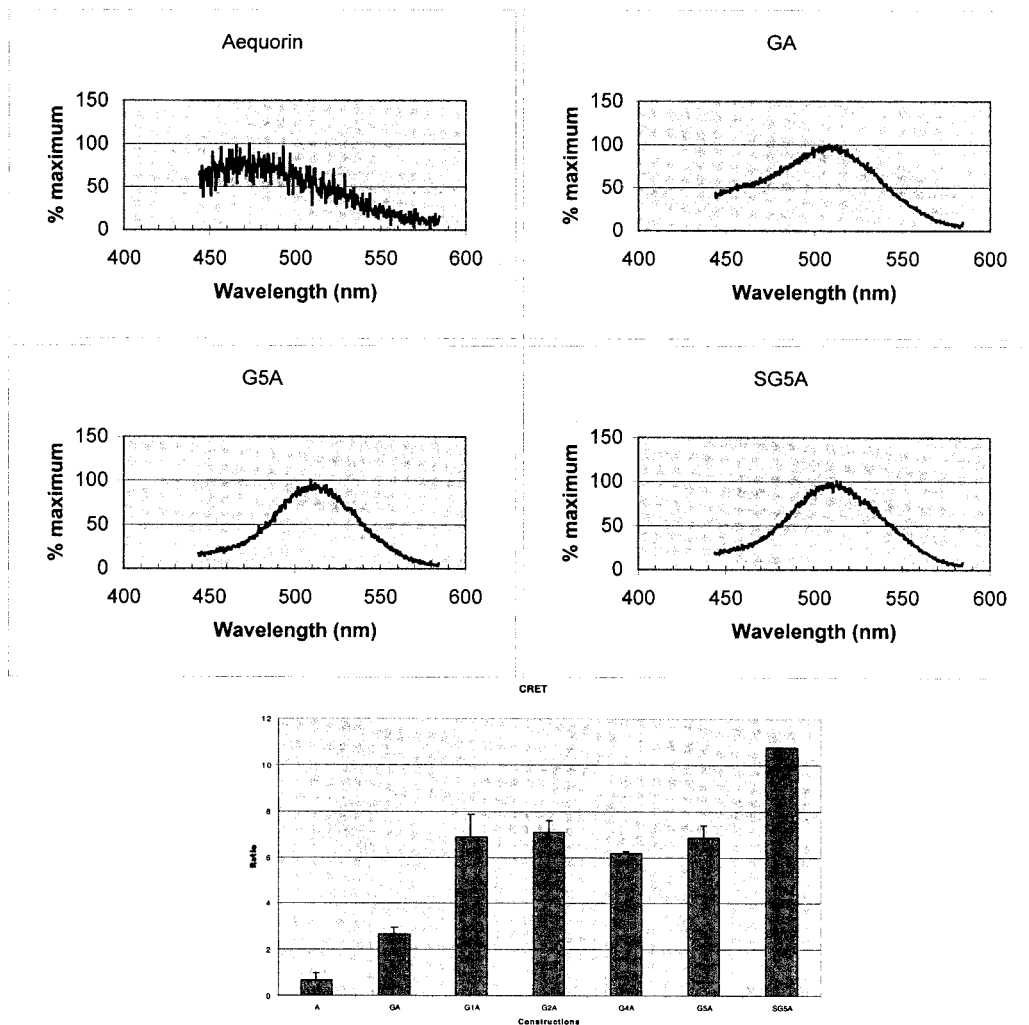


Fig. 2. Ca^{2+} CRET activities on cellular extracts. Emission spectra of aequorin and several GFP-aequorin fusion proteins were calibrated as a percentage of maximum intensity. CRET measurements are expressed as the ratio of green (500 nm) over blue (450 nm) photons.

bioluminescent marker is held back in the plasma membrane but nevertheless labels all neurite outgrowths present in Neuro2A cells.

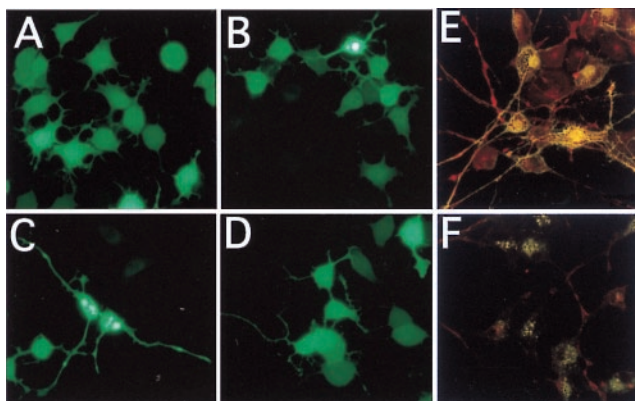


Fig. 3. GFP fluorescence of GFP-apoaequorin proteins in Neuro2A cells transfected with pGm (A), pGA (B), pG2A (C), and pG5A (D). Confocal superposition of GFP fluorescence and immunostaining of synaptotagmin in cells expressing either pSG5A (E) or pStG5A (F).

Ca^{2+} Detection in Single Cells. Neuro2A cells were transiently transfected with pA, pGA, pG2A, and pG5A or cotransfected with pA and pGm (Fig. 1). After aequorin reconstitution with native coelenterazine in Ca^{2+} -free buffer, an emission of photons has been measured with a classical intensified CCD camera upon the addition of CaCl_2 solution (5 mM) (Fig. 4A.1 and 4A.4). With the negligible background (Fig. 4A.2), integration time of 1 sec is enough to record the signal in single cells (Fig. 4A.1) expressing any of the fusion proteins. No signal could be visualized with aequorin alone or with coexpressed free GFP (data not shown). The presence of unbound GFP does not improve aequorin chemiluminescence as we observed *in vitro*. Because of the low level of light produced, aequorin expressed *in situ* has never been detected in single cells except when targeted in mitochondria. With a cooled intensified CCD camera, Rutter *et al.* (27) succeeded in detecting intramitochondrial Ca^{2+} signals when aequorin is fused to cytochrome *c* oxidase. Transgenes encoding cytoplasmic aequorin can report calcium activities in monolayers of cells only when photomultipliers are used, which are more sensitive but lack the spatial resolution for single-cell analysis. The stability of our GFP-aequorin fusions and the improved light emission have allowed us to detect physiological Ca^{2+} signals at the level of single cells.

Calcium deficiency before measurements or the transfection

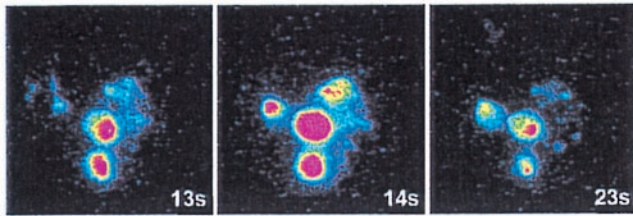
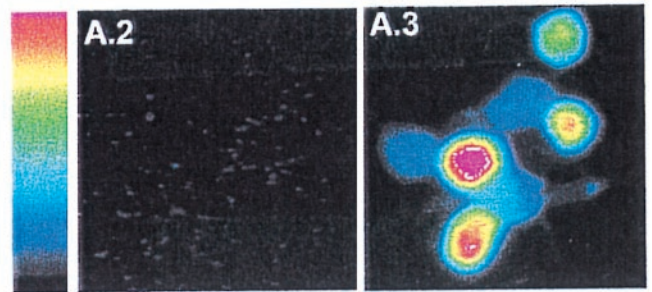
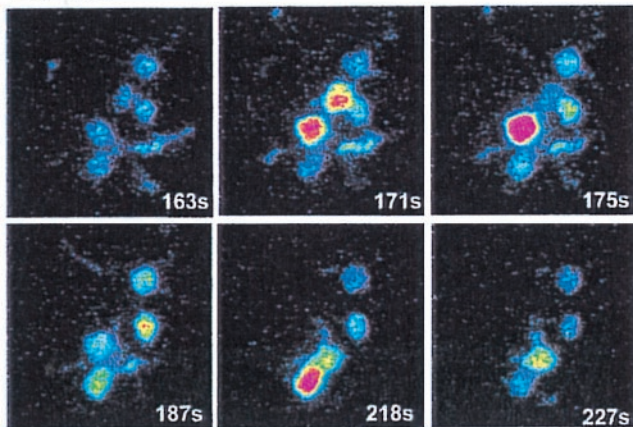
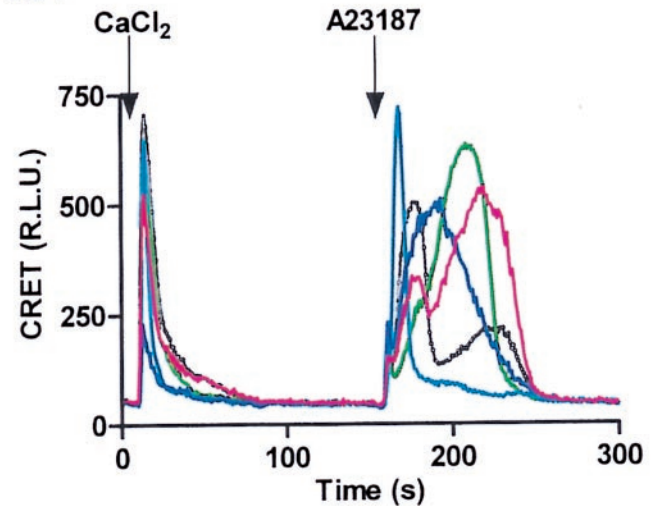
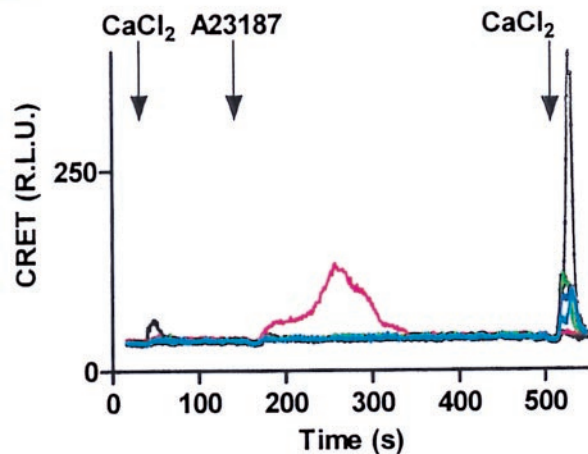
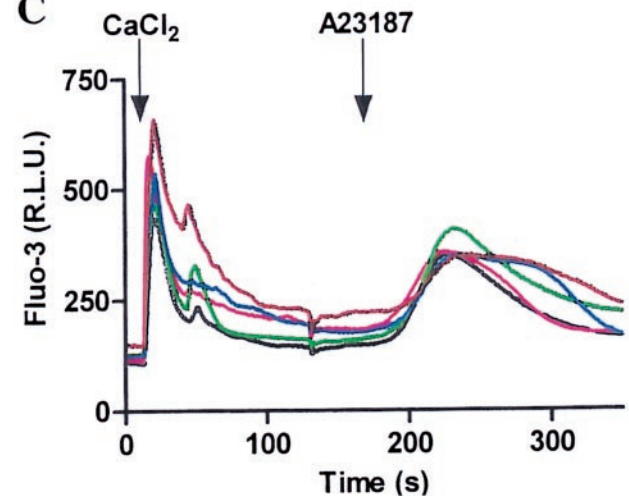
A.1**CaCl₂****A23187****A.4****B****C**

Fig. 4. Ca²⁺-induced bioluminescence was detected at the single-cell level. Neuro2A cells transfected with pGA (A. 1–A.4) or pSG5A (B) were preincubated with 5 μM coelenterazine in a Ca²⁺-free buffer (A.3). GFP fluorescence made it possible to choose transfected cells. The background recorded before CaCl₂ addition (A.2) corresponds to the RLU level at time 0 of the experiment (A.4 and B). Intensities of fluorescence and bioluminescence activity are translated in scaled pseudocolors. Representative pictures of the chosen field are shown after addition of 5 mM CaCl₂ and 5 μM A23187 at 13 sec and 159 sec, respectively, after the beginning of the acquisition (A.1 and A.4). Each profile indicates the intensity of light emitted by a single cell. We defined five regions of interest by encircling individual cell soma. With pGA (data not shown) or pSG5A (B) transfection, a high concentration of CaCl₂ (100 mM) was added at the end of the experiment (500 sec) to determine whether the bioluminescent protein was still active (C). Control experiments were made with Fluo-3 AM on mock-transfected Neuro2A cells.

conditions used may induce cellular depolarization, such that opening of the voltage-dependent Ca²⁺ channels is likely to be responsible for the fast bioluminescent response to CaCl₂ addition (Fig. 4A.4). Light emission then would return to background level because of the desensitization of Ca²⁺ channels and the membrane depolarization by Ca²⁺-dependent K⁺ channels (28).

Fluo-3 showed a similar profile in mock transfections of Neuro2A cells (Fig. 4C). Subsequent addition of a Ca²⁺ ionophore (A23187) induced a second emission of photons with comparable intensity but with different kinetics. A lower light intensity is detectable in Neuro2A cells transfected with pSG5A (Fig. 4B). When a fluorescent calcium probe is anchored to the

inner surface of the membrane, the response kinetics are much quicker than when the probe is not targeted (29). The use of the bioluminescent reporter SG5A probably requires a system with higher spatial and temporal resolutions. In any case, the responses observed are not caused by the complete consumption of aequorin as more bioluminescence can still be observed when a concentrated Ca^{2+} solution (100 mM) is applied to cells (see Fig. 4B for example). For each construction, measurements have been repeated at least four times. We observed a variability of individual cell responses probably because of cell population heterogeneity. Further investigations are required to calibrate RLU versus Ca^{2+} concentrations. Patch-clamp techniques also will allow the identification of the type of calcium channels implicated in these responses and the effect of cellular transfection on membrane potential.

The transgenes we have developed should permit imaging of electrical activity in neural networks in whole animals. *In vitro*, two approaches were used until recently. The first method is based on the coupling of exocytosis to emission of light from synaptolucins in nerve cells (30). Light emission occurs when the luciferase, targeted inside the synaptic vesicles, reacts with ATP in the extracellular space. With this system, the authors obtained signals correlated with the neurotransmitter release but the low light level requires very long acquisition times (over 30 sec). In the second approach, fluorescence Ca^{2+} -sensitive markers have been used for measurements of intracellular Ca^{2+} concentration by fluorescence resonance energy transfer (3, 4, 31). For single-cell detection, this technique requires a sufficient concentration of probe to discriminate the signal from the background that is generated by autofluorescence of biological compounds and the possibility of calcium-independent energy transfer between the

two GFPs. The integration times are also relatively long, between 4 and 20 sec.

In conclusion, we have elaborated bifunctional hybrids in which expression patterns can be followed by GFP fluorescence while the aequorin moiety is the reporter of Ca^{2+} activity. Furthermore, the functional coupling of the two components, which follows the CRET principle, results in a higher amount of light emission and a greater Ca^{2+} sensitivity. Bioluminescent activities of these genetic markers have been assessed in single cells with a cooled intensified CCD camera in 1-sec integration times. The recent development of low-level light detection systems should allow detection of CRET signals with much shorter integration times and higher spatial resolution. Intracellular and intercellular Ca^{2+} signaling could be approached *in vivo* in transgenic animals in which the GFP-aequorin is targeted to a particular cell population and/or to specific subcellular compartments. Particularly, calcium oscillations then could be imaged simultaneously in cells of an integrated neural circuitry in real time.

We thank Marie-Thérèse Nicolas for helpful discussions and the aequorin plasmid, Mitsunori Fukuda for the synaptotagmin I plasmid, Raymond Hellio and Jean-Claude Bénichou for their expert assistance with confocal and epifluorescence microscopy analysis, Gérard Baux and Jacques Stinnakre for helpful discussions, and Margaret Buckingham for critical reading of the manuscript. This work was supported by grants from the European Commission (CT 96-0378), the Association Française contre les Myopathies, and the Centre National de la Recherche Scientifique. V.B. was a recipient of grants from the IPSEN (Institut de Produits de Synthèse et d'Extraction Naturelle) Foundation and the Association Française contre les Myopathies.

- Berridge, M. J. (1998) *Neuron* **21**, 13–26.
- Cobbold, P. H. & Rink, T. J. (1987) *Biochem. J.* **248**, 313–323.
- Miyawaki, A., Griesbeck, O., Heim, R. & Tsien, R. Y. (1999) *Proc. Natl. Acad. Sci. USA* **96**, 2135–2140.
- Romoser, V. A., Hinkle, P. M. & Persechini, A. (1997) *J. Biol. Chem.* **272**, 13270–13274.
- Inoué, S., Noguchi, M., Sakaki, Y., Takagi, Y., Miyata, T., Iwanaga, S., Miyata, T. & Tsuji, F. I. (1985) *Proc. Natl. Acad. Sci. USA* **82**, 3154–3158.
- Prasher, D., McCann, R. O. & Cormier, M. J. (1985) *Biochem. Biophys. Res. Commun.* **126**, 1259–1268.
- Tsuji, F. I., Inoué, S., Goto, T. & Sakaki, Y. (1986) *Proc. Natl. Acad. Sci. USA* **83**, 8107–8111.
- Shimomura, O. & Johnson, F. H. (1978) *Proc. Natl. Acad. Sci. USA* **75**, 2611–2615.
- Sala-Newby, G. B., Badminton, M. N., Evans, W. H., Georges, C. H., Jones, H. E., Kendal, J. M., Ribeiro, A. R. & Campbell, A. K. (2000) *Methods Enzymol.* **305**, 479–498.
- Shimomura, O., Johnson, F. H. & Saiga, Y. (1962) *J. Cell Comp. Physiol.* **59**, 223–239.
- Johnson, F. H., Shimomura, O., Saiga, Y., Gershman, L. C., Reynolds, G. T. & Waters, J. R. (1962) *J. Cell Comp. Physiol.* **60**, 85–103.
- Cubitt, A. B., Heim, R., Adams, S. R., Boyd, A. E., Gross, L. A. & Tsien, R. Y. (1995) *Trends Biochem. Sci.* **20**, 448–455.
- Ward, W. W. & Cormier, M. J. (1976) *J. Phys. Chem.* **80**, 2289–2291.
- Ward, W. W. & Cormier, M. J. (1978) *Photochem. Photobiol.* **27**, 389–396.
- Morise, H., Shimomura, O., Johnson, F. H. & Winant, J. (1974) *Biochemistry* **13**, 2656–2662.
- Campbell, A. K. (1988) *Chemiluminescence: Principles and Application in Biology and Medicine* (Ellis Horwood, Chichester, U.K.), pp. 474–534.
- Cormack, B. P., Valdivia, R. H. & Falkow, S. (1996) *Gene* **173**, 33–38.
- Cramer, A., Whitehorn, E. A., Tate, E. & Stemmer, W. P. C. (1996) *Nat. Biotechnol.* **14**, 315–319.
- Siemering, K. R., Golbik, R., Sever, R. & Haseloff, J. (1996) *Curr. Biol.* **6**, 1653–1663.
- Watkins, N. J. & Campbell, A. K. (1993) *Biochem. J.* **293**, 181–185.
- Badminton, M. N., Sala-Newby, G. B., Kendall, J. M. & Campbell, A. K. (1995) *Biochem. Biophys. Res. Commun.* **217**, 950–957.
- Morin, J. G. & Hastings, J. W. (1970) *J. Cell. Physiol.* **77**, 313–318.
- Campbell, A. K. & Hallett, M. B. (1978) *Proc. Physiol. Soc.* **287**, 4–5.
- Yang, F., Moss, L. G. & Phillips, G. N., Jr. (1996) *Nat. Biotechnol.* **14**, 1246–1251.
- Brose, N., Petrenko, A. G., Südhof, T. C. & Jahn, R. (1992) *Science* **256**, 1021–1025.
- Coco, S., Verderio, C., De Camilli, P. & Matteoli, M. (1998) *J. Neurochem.* **71**, 1987–1992.
- Rutter, G. A., Burnett, P., Rizzuto, R., Brini, M., Murgia, M., Pozzan, T., Tavaré, J. M. & Denton, R. M. (1996) *Proc. Natl. Acad. Sci. USA* **93**, 5489–5494.
- Sah, P. (1996) *Trends Neurosci.* **19**, 150–154.
- Etter, E. F., Minta, A., Poenie, M. & Fay, F. S. (1996) *Proc. Natl. Acad. Sci. USA* **93**, 5368–5373.
- Miesenböck, G. & Rothman, J. E. (1997) *Proc. Natl. Acad. Sci. USA* **94**, 3402–3407.
- Miyawaki, A., Llopis, J., Heim, R., McCaffery, J. M., Adams, J. A., Ikura, M. & Tsien, R. Y. (1997) *Nature (London)* **388**, 882–887.